

# Growth of Helium Shells inside Spherical Adsorbers

E. S. Hernández

*Departamento de Física, Facultad de Ciencias Exactas y Naturales,  
Universidad de Buenos Aires, 1428 Buenos Aires,  
and Consejo Nacional de Investigaciones Científicas y Técnicas, Argentina*

*The adsorption of helium on spherical cavities is investigated employing finite range density functional theory. It is known that for films outside spherical walls, a growth instability occurs above a critical film thickness. This instability may be overcome by stable capillary condensation inside the gap between an inner sphere and an outer spherical cavity bounded by spherical graphene, metallic sheets and voids in bulk metals. When a C<sub>60</sub> fullerene is placed at the center of the spherical well, one can observe the competition between the formation of helium shells on the walls and the attraction of the opposite adsorbing field.*

*PACS numbers 67.60.-g, 67.70.+n, 61.46.+w*

## 1. INTRODUCTION

Helium films on adsorbing surfaces constitute quasi-twodimensional non-homogeneous fluids, whose zero temperature energetics, structure and growth pattern have been investigated from microscopic and from semiphenomenological viewpoints<sup>1</sup>. In particular, finite range density functional (FRDF) theory is a useful tool to advance several characteristics of confined helium fluids, especially in configurations that prevent rigorous microscopic calculations. Shortly ago, we have considered the possibility of helium adsorption on the outer surface of carbon fullerenes<sup>2</sup> and spheres coated with weaker adsorbers such as Mg, Li and Cs<sup>3</sup>. These systems exhibit an important property of adsorption on curved surfaces, such as the appearance of a spinodal-like instability above a few helium layers, indicating that thick fluid shells cannot support fluctuations in the number of adsorbed atoms. This growth instability originates in the increase of the areal free energy at the liquid-vapor

interface with the outer radius of the film, which in turn sets a limit to the system's capacity to incorporate extra material.

Very recently, it has been shown that this unstable growth can be counteracted by capillary condensation (CC) between neighbouring adsorbers in an array of metallic wires<sup>4</sup>. In the same philosophy, in this paper I investigate the systematics of <sup>4</sup>He shells inside spherical gaps at zero temperature in the FRDF frame, focusing on the competition between unstable film growth on a sphere and stable CC in an collection of surrounding spherical adsorbers. As in ref. 4, a simplified mean field-like model is employed, assuming that each ball experiences the influence of the environment as if it consisted of either a concentric spherical sheet or a void in bulk metal. The results here presented illustrate adsorption in the gap between a cavity and an inner concentric  $C_{60}$  fullerene.

## 2. ADSORPTION OF HELIUM INSIDE SPHERICAL GAPS

Within FRDF, one can derive the equation of state of  $N$  helium atoms inside a spherical cavity of radius  $R$ . One starts from an energy density  $\mathcal{E}[\rho(\mathbf{r})]$ , where  $\rho(\mathbf{r})$  is the particle density, normalized to the total number of helium atoms. The integrodifferential Euler-Lagrange equation is derived by functional differentiation of the total energy with respect to  $\rho$ , and takes the form

$$\left[ -\frac{\hbar^2}{2m_A} \nabla^2 + U(\rho) + V(\mathbf{r}) \right] \sqrt{\rho(\mathbf{r})} = \mu \sqrt{\rho(\mathbf{r})} \quad (1)$$

with  $\mu$  the <sup>4</sup>He chemical potential,  $U(\rho)$  the density-dependent mean field and  $V(\mathbf{r})$  the adsorbing potential. To derive the expression of  $V(\mathbf{r})$ , one considers one helium atom at radial distance  $r$  inside/outside a spherical sheet with areal density  $\rho(r) = \rho_0 \delta(R - r)$ , or in a cavity in bulk material of uniform density  $\rho(r) = \rho_0 \Theta(R - r)$ . The adatom interacts pairwise with atoms in the adsorber via a Lennard-Jones potential of strength  $\epsilon$  and core radius  $\sigma$ , so that the overall field at point  $r$  can be obtained by angular integration, plus a radial integration up to infinity in the case of a cavity. The final expressions are given in ref. 2 for the inner and outer fields of a spherical sheet, and in ref. 5 for a spherical void inside a solid.

Equation (1) is solved numerically<sup>2,3</sup> to obtain the chemical potential, the total energy, the grand potential per particle  $\Omega/N = E/N - \mu$  and the density profiles  $\rho(r)$ , as functions of the number of helium atoms. The FRDF is the same employed to investigate the growth of <sup>4</sup>He shells on spherical fullerenes<sup>2,3</sup> and inside cylindrical gaps<sup>4</sup>. Following ref. 4, we adopt a simple model, that simulates the influence of an environment consisting of a gas of spherical adsorbers on a helium film growing on a single  $C_{60}$  fullerene. In

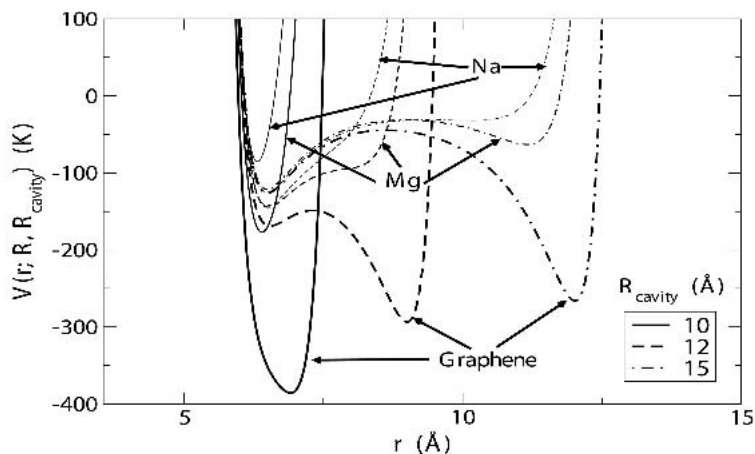


Fig. 1. Total adsorbing field of a  $C_{60}$  fullerene of radius  $3.55 \text{ \AA}$  concentric with outer cavities of radii 10, 12 and  $15 \text{ \AA}$ . Thick, intermediate and thin lines respectively depict a graphene sheet, a Mg foil and a void in metallic Na as external boundaries.

order to maintain the spherical geometry, the effect of surrounding balls is represented by a spherical cavity concentric with the fullerene; the  $^4\text{He}$  atoms thus form a shell bounded by two spherical surfaces. Fig. 1 shows the total adsorbing field  $V(r) = V_{C_{60}}(r) + V_{cavity}(r)$  for a spherical gap between a central fullerene of radius  $R = 3.55 \text{ \AA}$  and cavities of radii  $R_{cavity} = 10, 12$  and  $15 \text{ \AA}$  in the vicinity of the crossover from one to two minima. The thickest, intermediate and thin lines respectively correspond to graphene sheets, Mg sheets and to a spherical void in bulk Na<sup>5</sup>. We clearly appreciate the varying adsorbing power, from the very strong graphene to the weak solid Na, with Mg foil as an intermediate stage.

Figure 2 displays the  $^4\text{He}$  chemical potential in the above wells as a function of particle number. Atoms are unbounded between  $C_{60}$  and a void in solid Na with a radius of  $10 \text{ \AA}$  (not included). In all cases, submonolayer condensation takes place at relatively small particle numbers and as usual in these plots, abrupt changes in the slope of the curve  $\mu(N)$  indicate layering transitions. For the three adsorbing materials, we observe promotion to a second layer, that takes place for the 12 and  $15 \text{ \AA}$  graphene sheet and for the  $15 \text{ \AA}$  Mg and Na walls. A single monolayer is present in the  $10 \text{ \AA}$  graphene and Mg foils, and in the  $12 \text{ \AA}$  Mg and Na cavities, until the fluid exhausts the

We have verified that for small drops the exponential factor is preferable over the gaussian one which would be the corresponding to an harmonic confinement. On the other hand, we have also employed more complex forms for the dynamical part of  $f_2$  (models proposed for Reatto<sup>11</sup> and Lewerenz<sup>12</sup>) but without significant improvements in the binding energy.

The function  $\xi(r)$ , which models the strength of the triplet correlation (4), is a gaussian

$$\xi(r) = \exp \left[ - \left( \frac{r - r_t}{\omega_t} \right)^2 \right], \quad (7)$$

and the corresponding function for the backflow correlation (5) is also a gaussian plus a longer-range correction<sup>13</sup>

$$\eta(r) = \lambda_{bs} \exp \left[ - \left( \frac{r - r_B}{\omega_B} \right)^2 \right] + \frac{\lambda_{bl}}{r^3}. \quad (8)$$

The optimization of the parameters of  $\psi$  is carried out by searching for a minimum of the energy. This is done recursively, starting with the two-body factor and then improving the approximation. The best set of parameters at each level of correlations is reported in Table 1.

The VMC results obtained for the total and partial energies per particle are reported in Table 2. The total energy results from a big cancellation between the potential and kinetic energies and it is very small if compared, for instance, with the binding energy of bulk <sup>3</sup>He at equilibrium (-2.47 K). Starting with the simplest approximation (J), the introduction of triplet (T) and backflow (B) correlations separately improves the bound for the energy, with a larger effect in the case of backflow. Nevertheless, both J-T and J-BS are not enough to achieve a bound system. If on top of J-BS one introduces triplets, the drop becomes self-bound. Our best VMC energy is obtained by

Aprox.	$\alpha(\sigma^{-1})$	$b(\sigma)$	$\lambda_{bs}$	$\lambda_{bl}(\sigma^3)$	$\lambda_3(\sigma^{-2})$
J	4.4	1.14	0	0	0
J-T	4.4	1.14	0	0	-1.5
J-BS	4.4	1.14	0.34	0	0
J-BS-T	4.4	1.14	0.34	0	-1.5
J-BS-BL-T	4.4	1.14	0.14	0.077	-1.5

Table 1. Optimal values for the variational parameters entering  $\psi$  in the different approximations ( $\sigma = 2.556 \text{ \AA}$ ). J and T stand for Jastrow and triplet correlations; BS and BL for the short- and long range backflow terms, respectively. In Eq. (7),  $r_t = 0.66\sigma$  and  $\omega_t = 0.5\sigma$ . In Eq. (8),  $r_B = 0.75\sigma$  and  $\omega_B = 0.54\sigma$ .

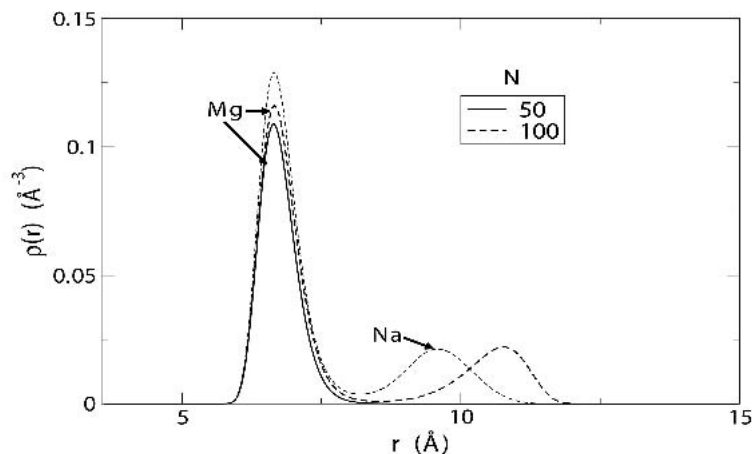


Fig. 3. Density profiles of the helium atoms in the  $C_{60}$ -15 Å Mg and Na gaps for 50 and 100 particles. For  $N = 50$ , the Mg and Na peaks are indistinguishable in the current scale.

on fullerenes and other coated spheres, provided that sufficiently large gaps appear to support CC. The model has already been tested in the cylindrical geometry and it has been shown that in spite of its crudeness, it may throw light on the basic physics. Starting from an established feature of curved substrates, namely the existence of a growth instability for helium films, we can see that CC counteracts this instability to different degrees. If the  $C_{60}$  molecule is in the presence of an outer graphene sheet, the mechanism is to shift the onset of adsorption from the central fullerene to the external wall. If the external boundary is metallic, either a Mg foil or a much weaker cavity in bulk Na, this extra adsorbing field is weaker than the fullerene's; consequently, its presence does not strongly compete with the layering tendency of the inner graphite sphere, but counteracts the growth instability by giving rise to finite storage capacity in the spherical gap. In all cases, the finite size of the gap between the two surfaces sets a limit to the amount of adsorbed material; if the distance between surfaces is large enough, the fluid can undergo CC, before expelling the excess into vapor.

Prior to this work, the effects of CC in curved pores have been investigated resorting to thermodynamical models<sup>5-7</sup>. In particular, in ref. 5 it is shown that the predictions of the simple model are consistent with FRDF

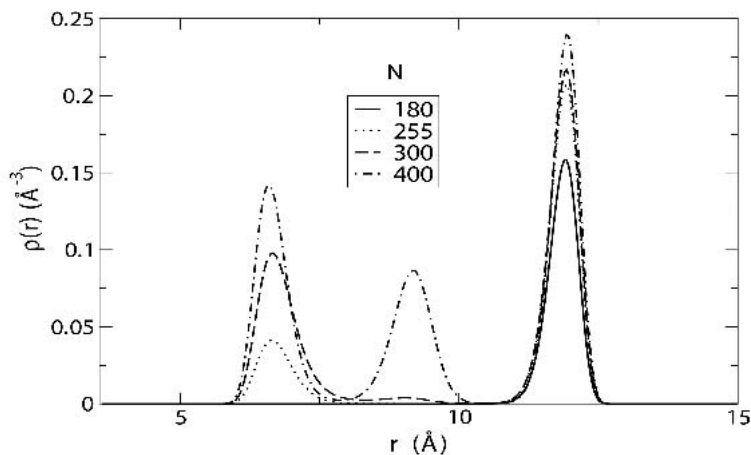


Fig. 4. Density profiles of the helium atoms in the  $C_{60}$ -15 Å graphene gap for various numbers of particles.

calculations.

### ACKNOWLEDGMENTS

This work was partially supported by grants PICT03-08450 (ANPCYT) PIP2391-00 and X103 (UBA) from Argentina.

### REFERENCES

1. *Microscopic Approaches to Quantum Liquids in Confined Geometries*, edited by E. Krotscheck and J. Navarro, World Scientific, Singapore (2002)
2. E. S. Hernández, M. W. Cole and M. Boninsegni, *Phys. Rev. B* **68**, 1254181 (2003).
3. E. S. Hernández, M. W. Cole and M. Boninsegni, *J. Low Temp. Phys.* **134**, 309 (2004).
4. E. S. Hernández, *J. Low Temp. Phys.*, in press.
5. I. Urrutia and L. Szybisz, to be published.
6. S. M. Gatica, M. M. Calbi and M. W. Cole, *Phys. Rev. B* **65**, 061605 (2002).
7. L. Szybisz and I. Urrutia, *Phys. Rev. E* **66**, 051201 (2002).